Energy as a global-scale diagnostic for MI coupling processes

Tuija I. Pulkkinen

IGPP / Los Alamos National Laboratory, NM

Permanently at: Finnish Meteorological Institute, Helsinki, Finland

Outline

Introduction to energy coupling

- Observational parameters
- Correlation studies

Introduction to MHD simulations

- GUMICS-4 global simulation
- Tracing energy in a simulation
- Analysis methods
- Relationship of energy transfer and reconnection

Results of simulation runs

- Magnetopause energy transfer
- Tail reconnection
- Ionospheric energy dissipation

Implications to MI coupling

- Role of dynamic pressure
- Substorm energetics

IMF control of substorm activity

Proxy for energy input:

- Epsilon-parameter

  $\varepsilon = (4\pi/\mu_0)vB^2 l_0^2 \sin^4(\theta/2)$

Proxy for auroral-latitude energy dissipation:

- AL index

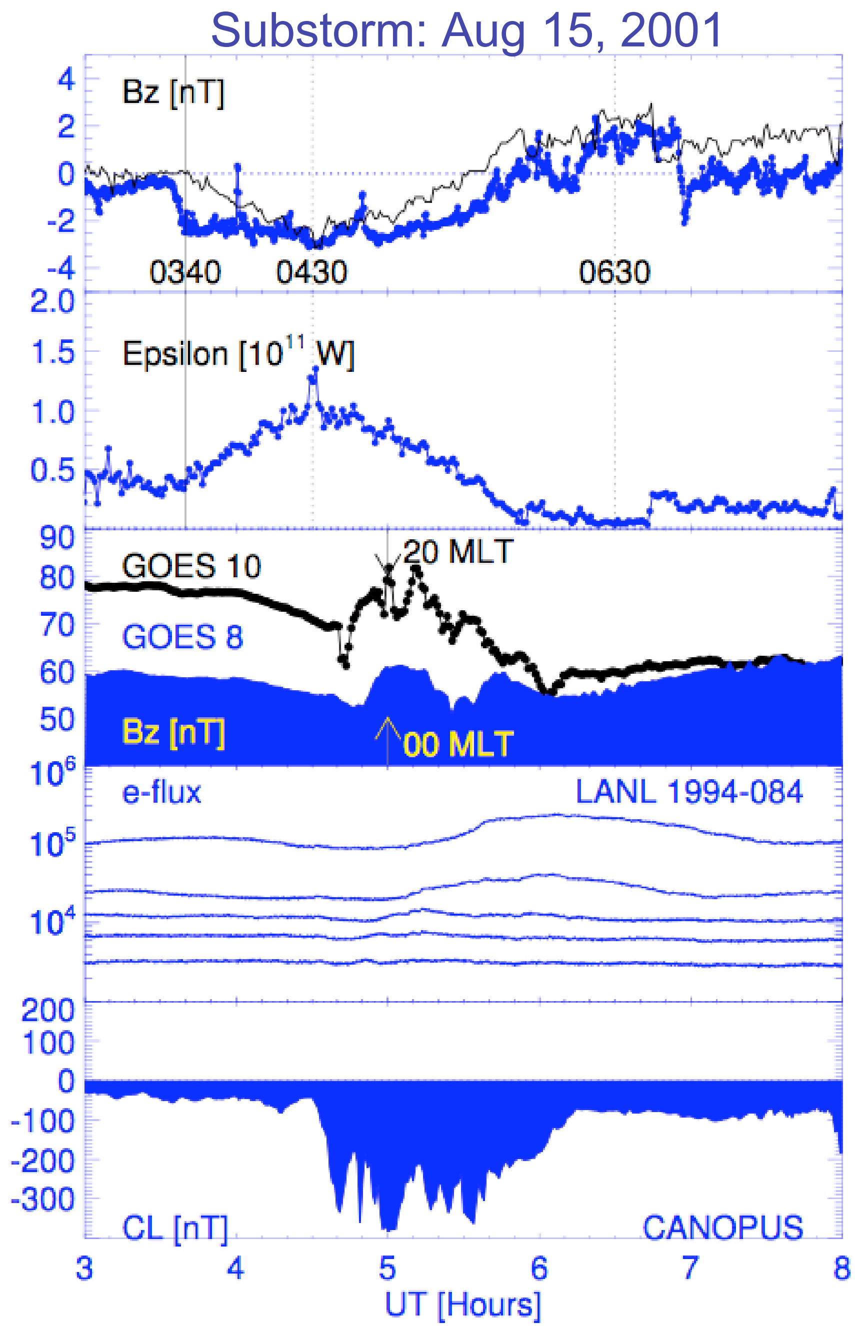

Energy input - output correlation

Estimate of energy dissipation in the ionosphere:

- Determine substorm onset and end of recovery phase times
- Integrate over time
  - Epsilon
  - AL

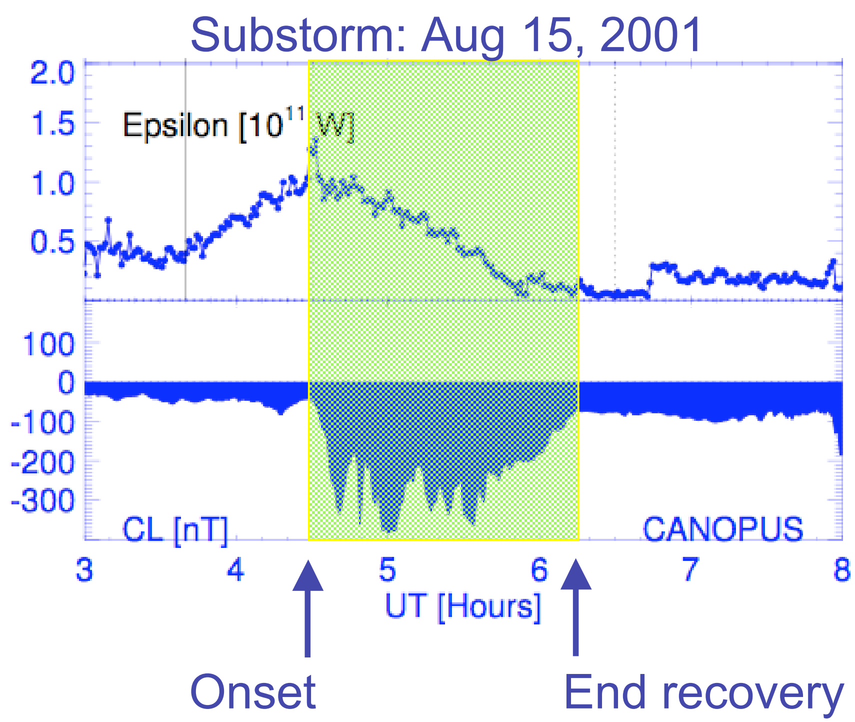

Energy input - output correlation

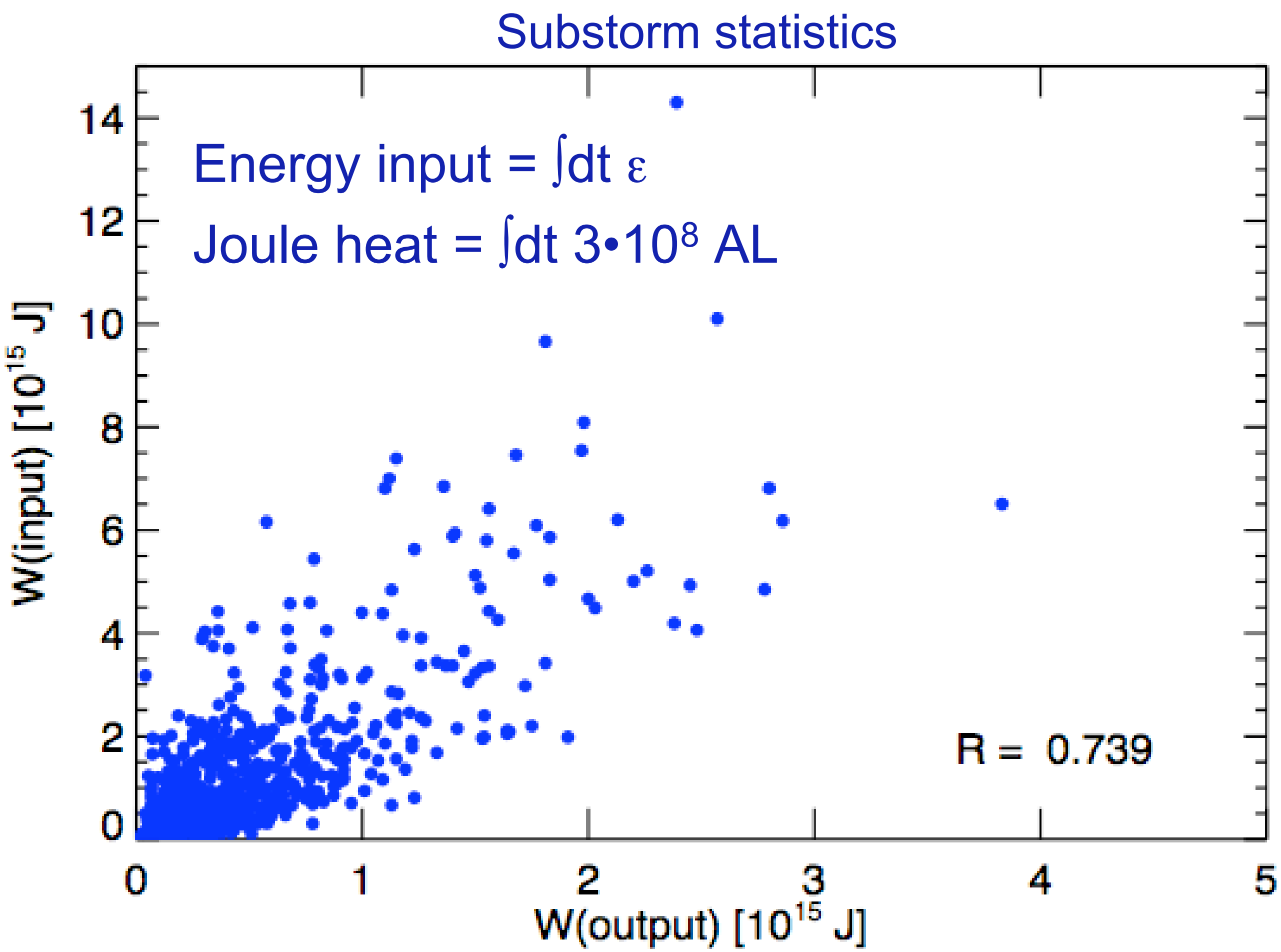

(*Tanskanen et al., 2001*)

IMF control of ring current activity

Proxy for energy input:

- Solar wind $E_Y = VB_s$

Proxy for ring current energy content:

- Mid-latitude Dst-index

Burton formulation:

$d\mathrm{Dst}^*/dt = Q(E_Y) - \mathrm{Dst}^*/\tau\ (E_Y)$

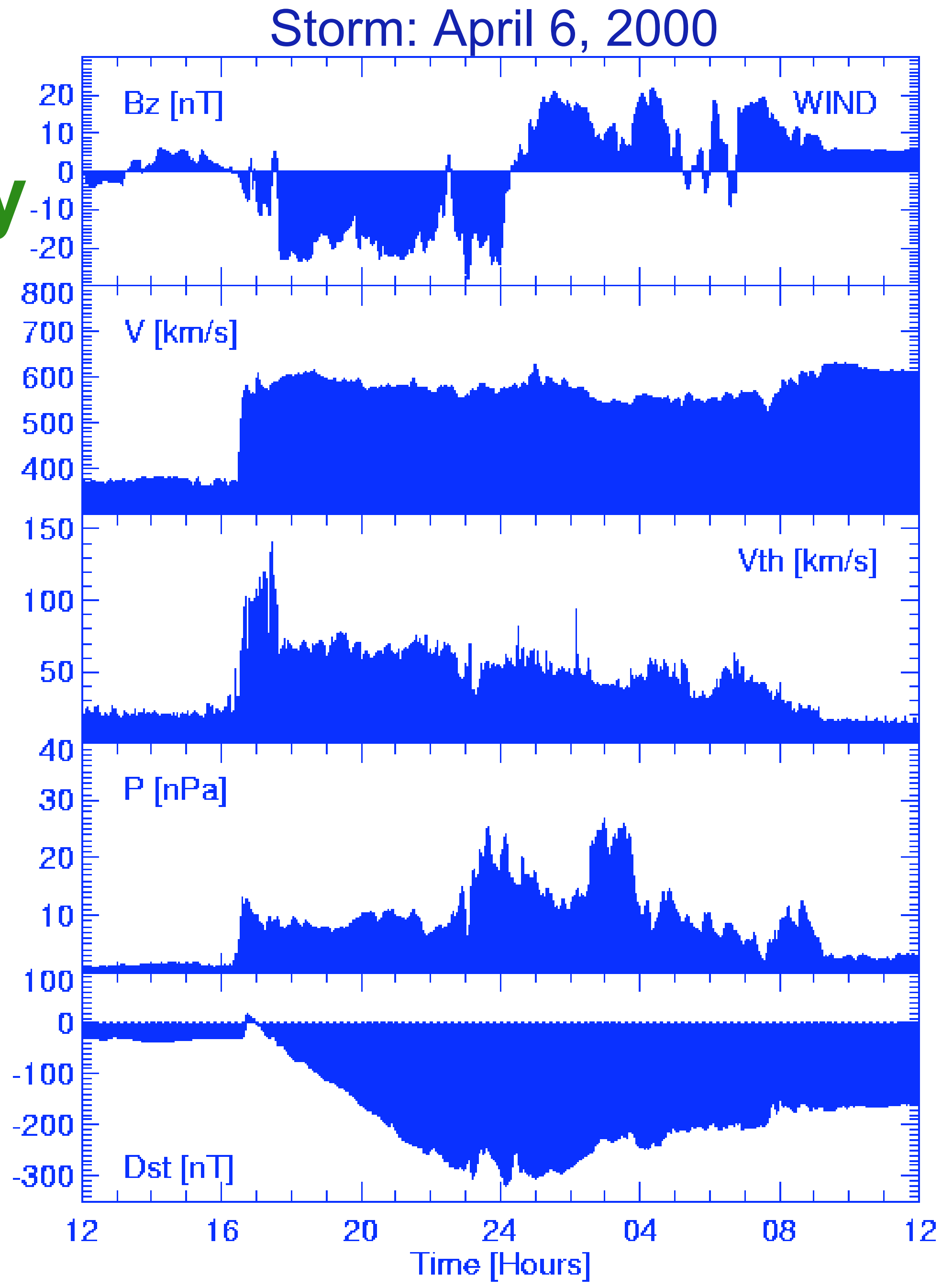

Importance of global modeling

- We want to trace the flow of energy, mass, and momentum from the Sun and the solar wind through the magnetosphere - ionosphere system

- Global observations almost non-existent
  - various proxies are available

- Global model results can be used to
  - compute global quantitites of energy and mass flow
  - compare with observational proxies

GUMICS-4: A global MHD simulation

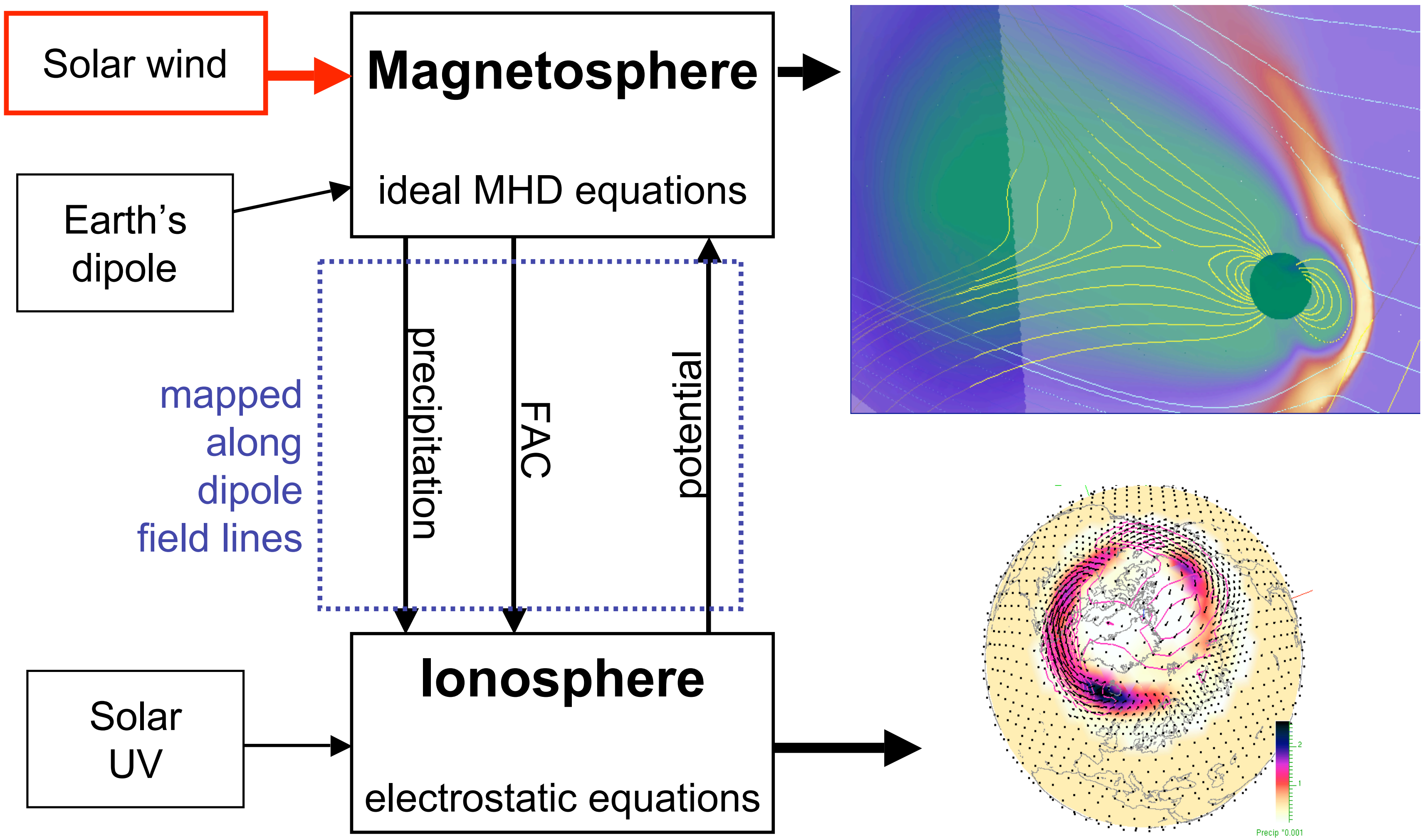

Magnetopause location

Automatic detection by using cavity carved by solar wind flow lines

- Agrees with previous definitions (current density, open-closed boundary)

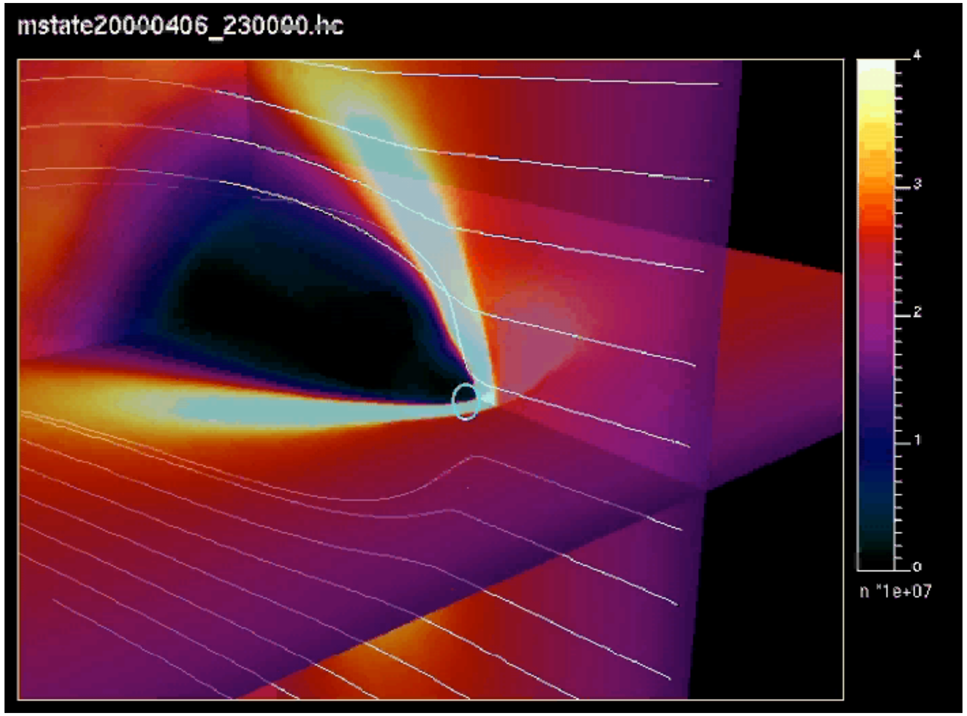

Poynting flux flow lines

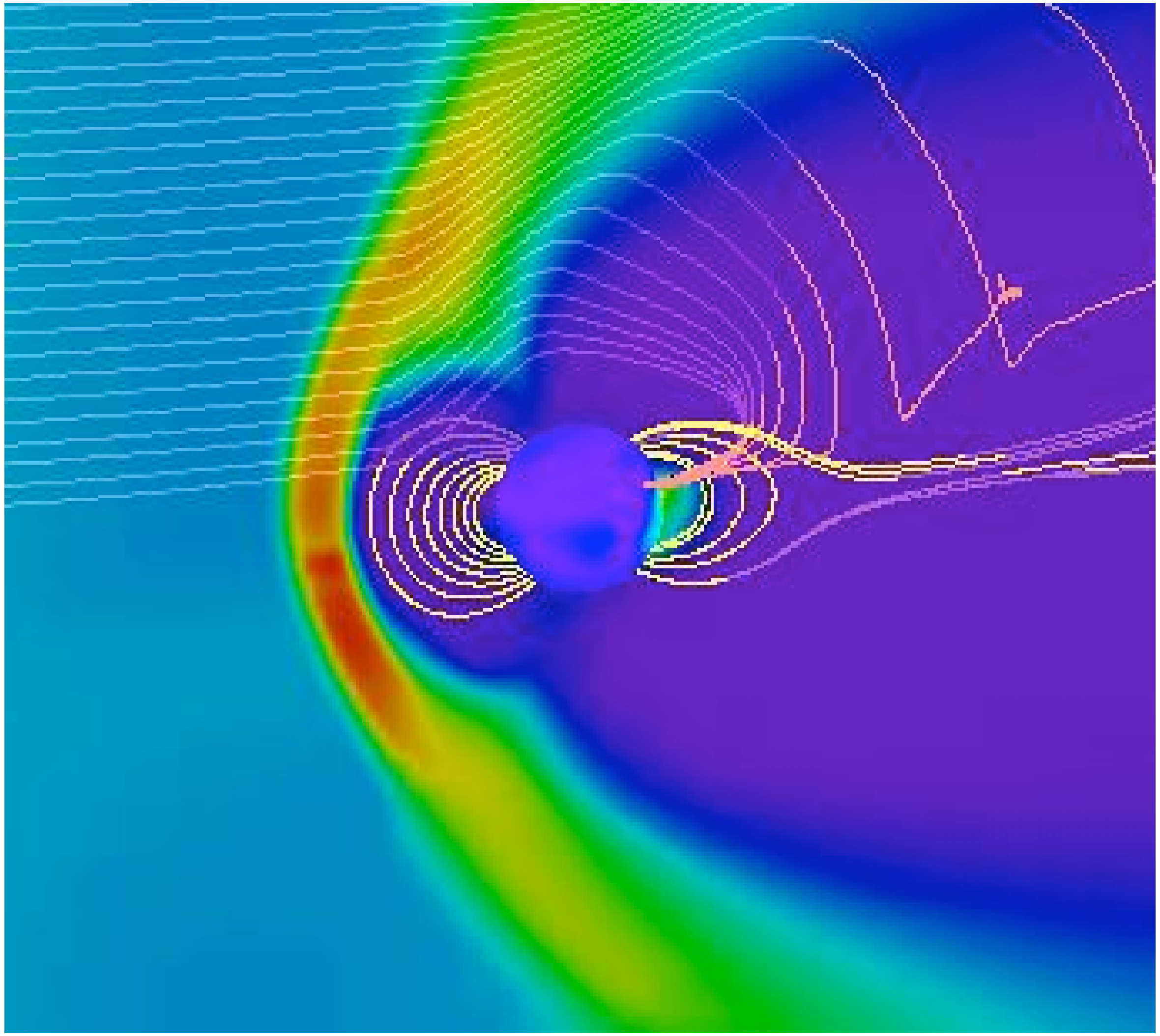

Energy and mass transfer through magnetopause

Storm: April 6, 2000

Total energy flux K:

$$E_S = \int dA \, \mathbf{K} \cdot \mathbf{n}$$

Mass flux ρV:

$$\rho V_S = \int dA \, \rho \mathbf{V} \cdot \mathbf{n}$$

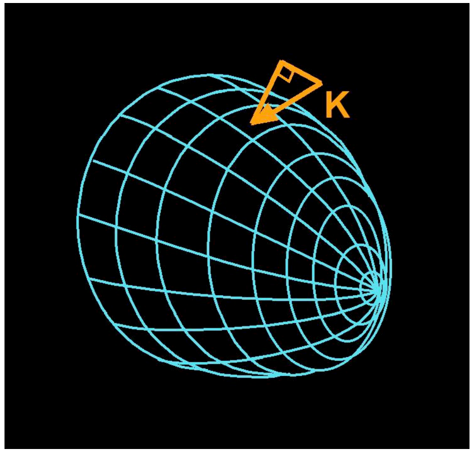

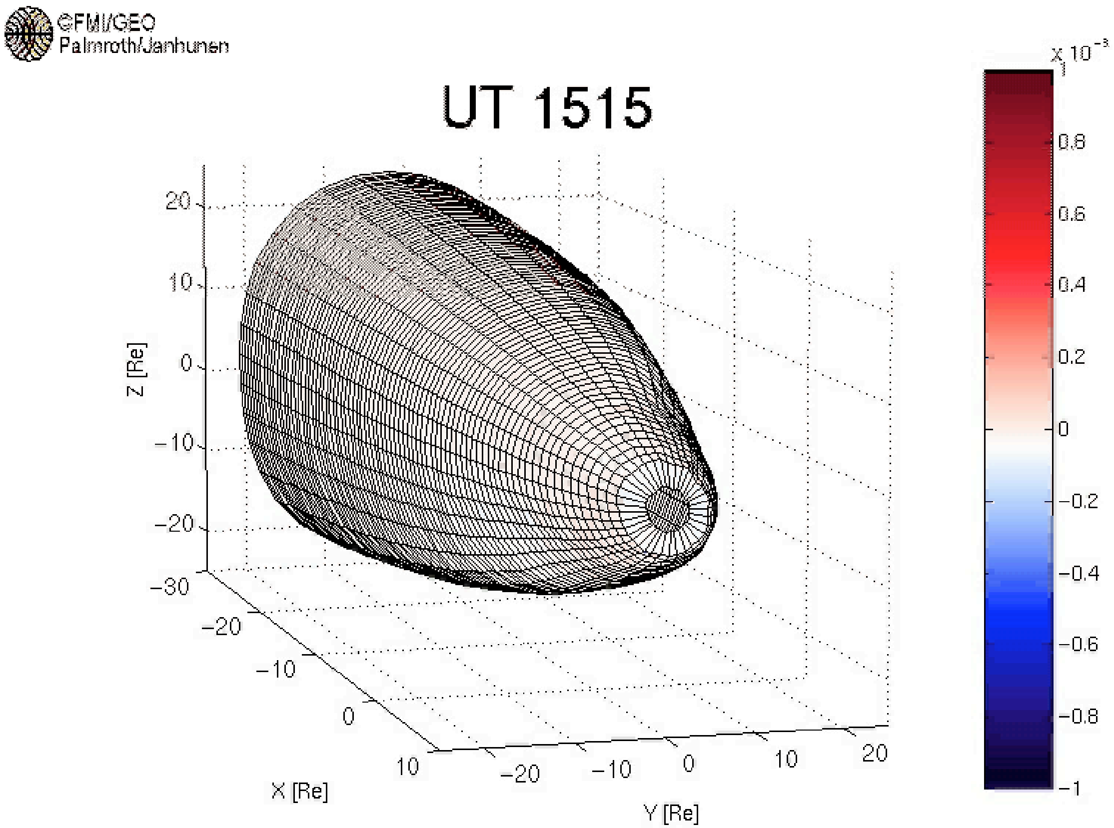

(Palmroth et al., 2003)

Energy through magnetopause: Comparison with empirical proxy

Energy input (Akasofu, 1981):

$$\varepsilon = (4\pi/\mu_0) v B^2 l_0^2 \sin^4(\theta/2)$$

- scale l_0 selected to equal inner magnetosphere dissipation
- ε need not be same as total energy flux through boundary

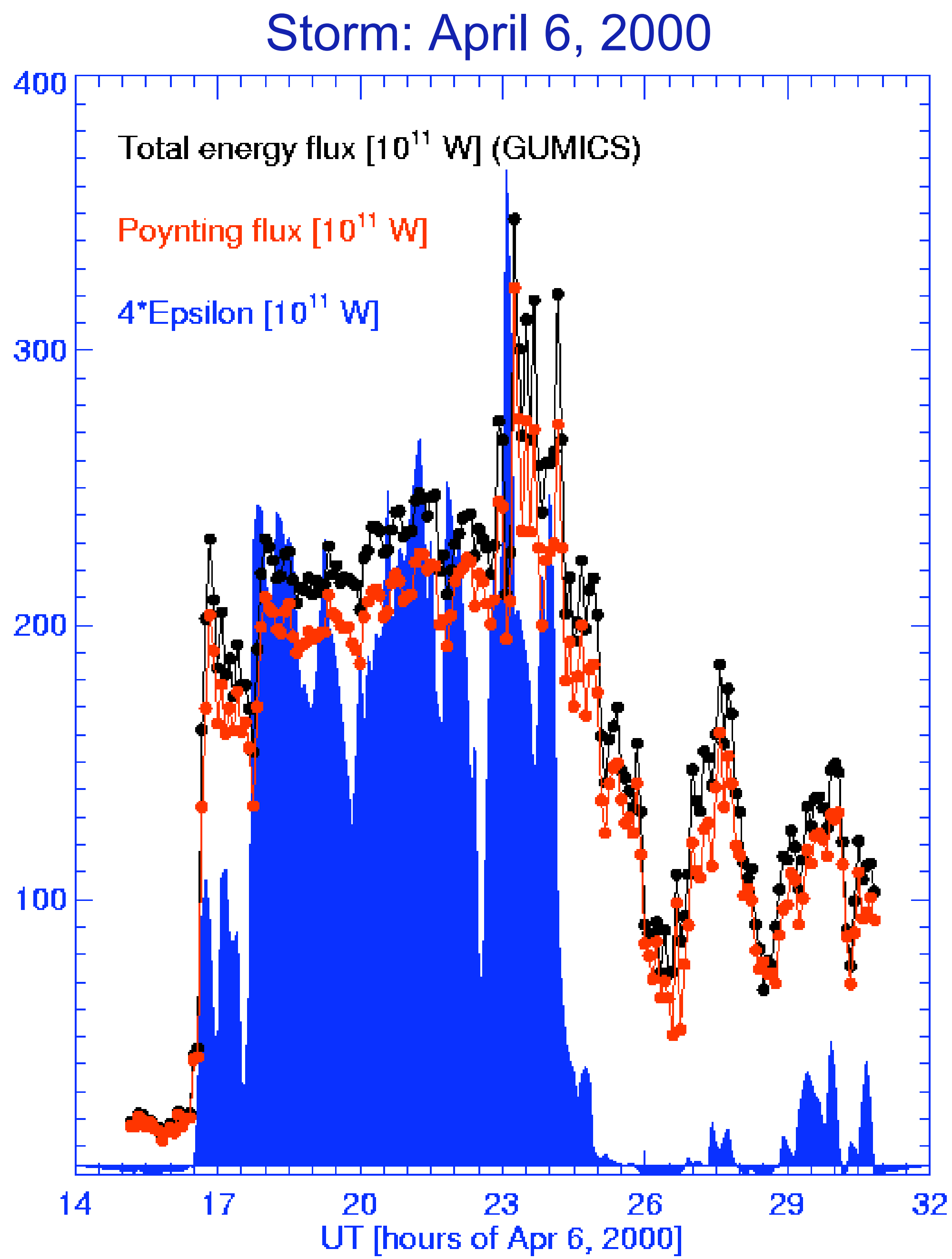

Reconnection in GUMICS-4

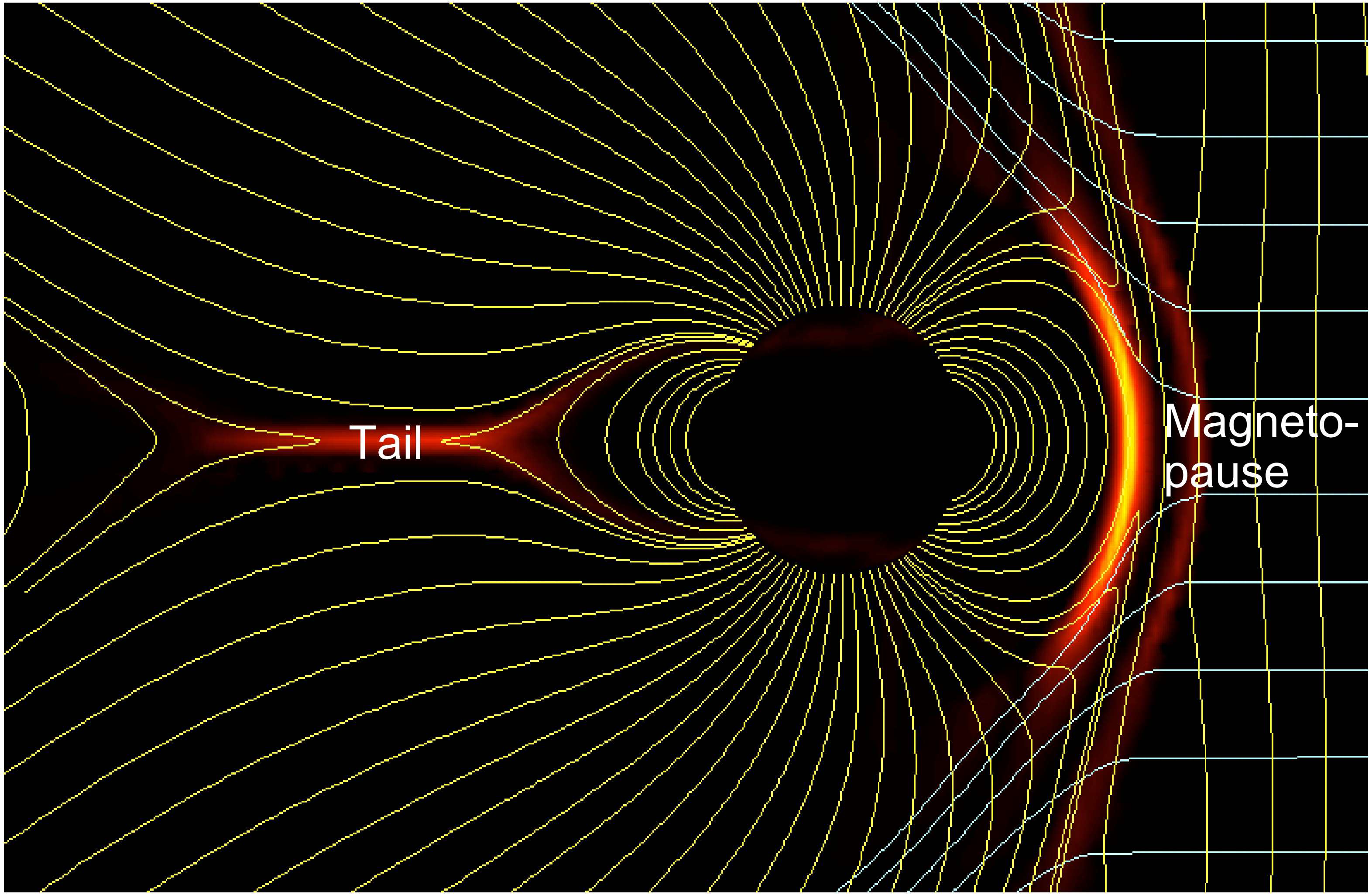

Different field line topologies

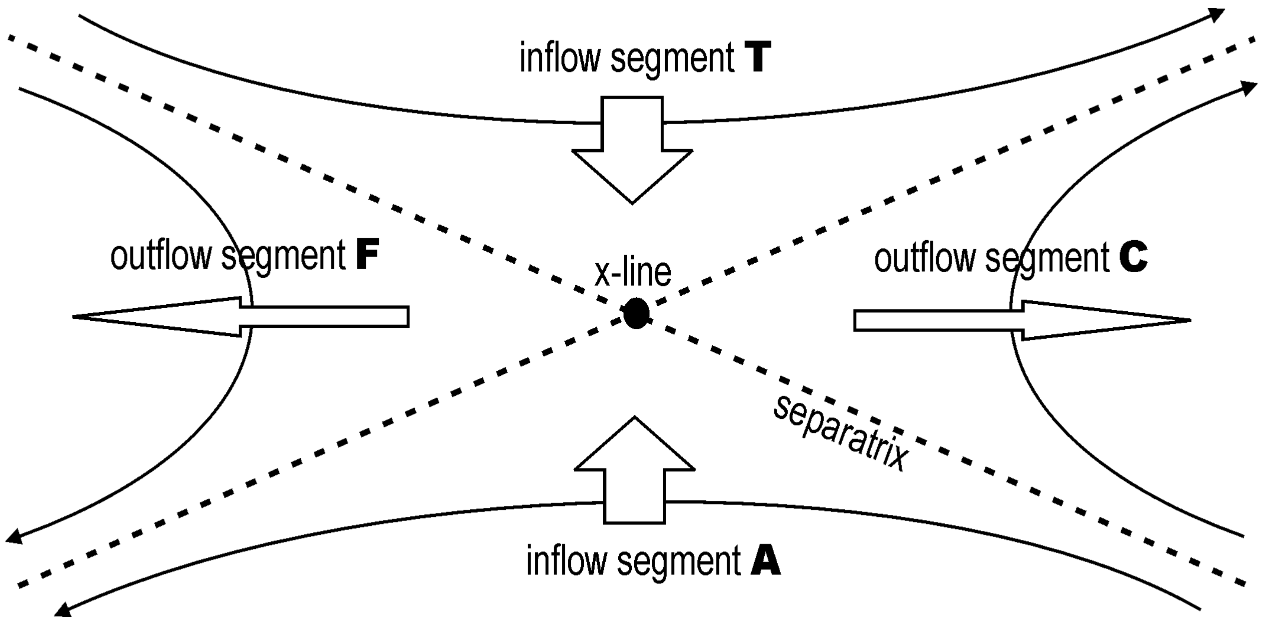

- Four distinct field line regions meet at the X-line

Different field line topologies

Field lines in the magnetosphere:

- Free
- Closed
- Open, Toward Earth
- Open, Away from Earth

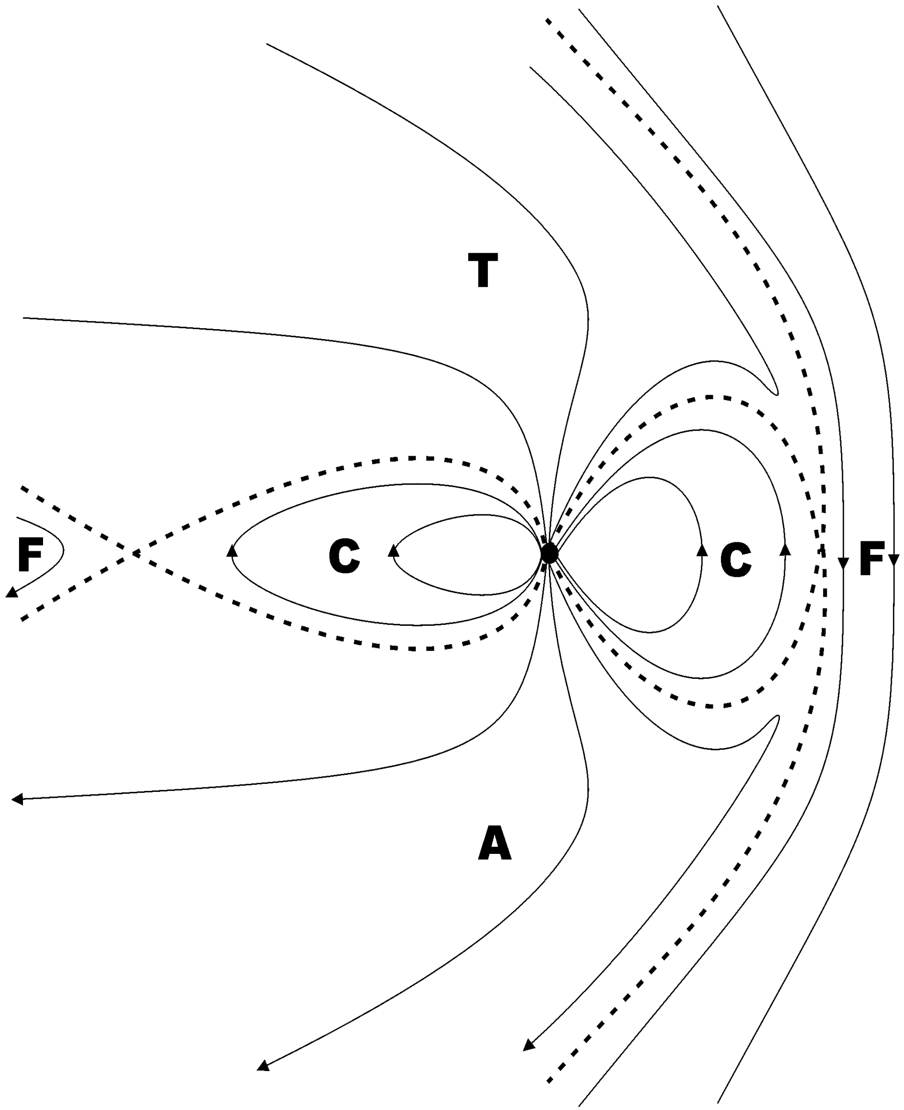

Identifying reconnection

Traditional measure parallel electric field not optimal:

- Ideal MHD has no parallel electric fields

  $\mathbf{E} = -\mathbf{v} \times \mathbf{B}; \quad E_{||} = 0$

- $\mathbf{E}_{||}$ depends on resistivity not well understood in space plasmas
- Gradients at the X-line are large and numerical effects from discretization in simulations may be significant

Look for characterizations not localized to the X-line:

- Reconnection occurs where all four types of field lines are found

Reconnection sites

Colored lines:

- Locations where four field line topologies are found within three grid points

Green thin line:

- Tail X-line as identified from Bx reversal

Reconnection definitions agree

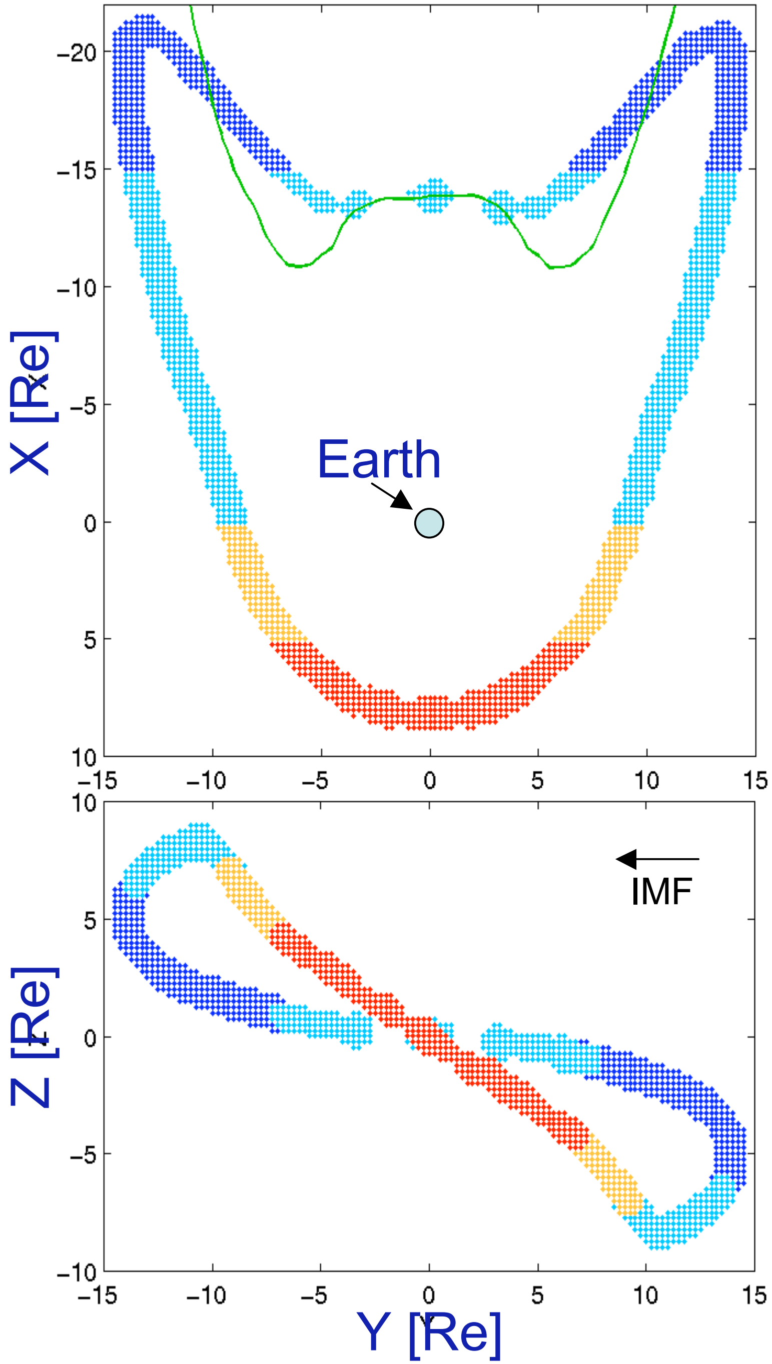

Dayside reconnection sites follow IMF direction

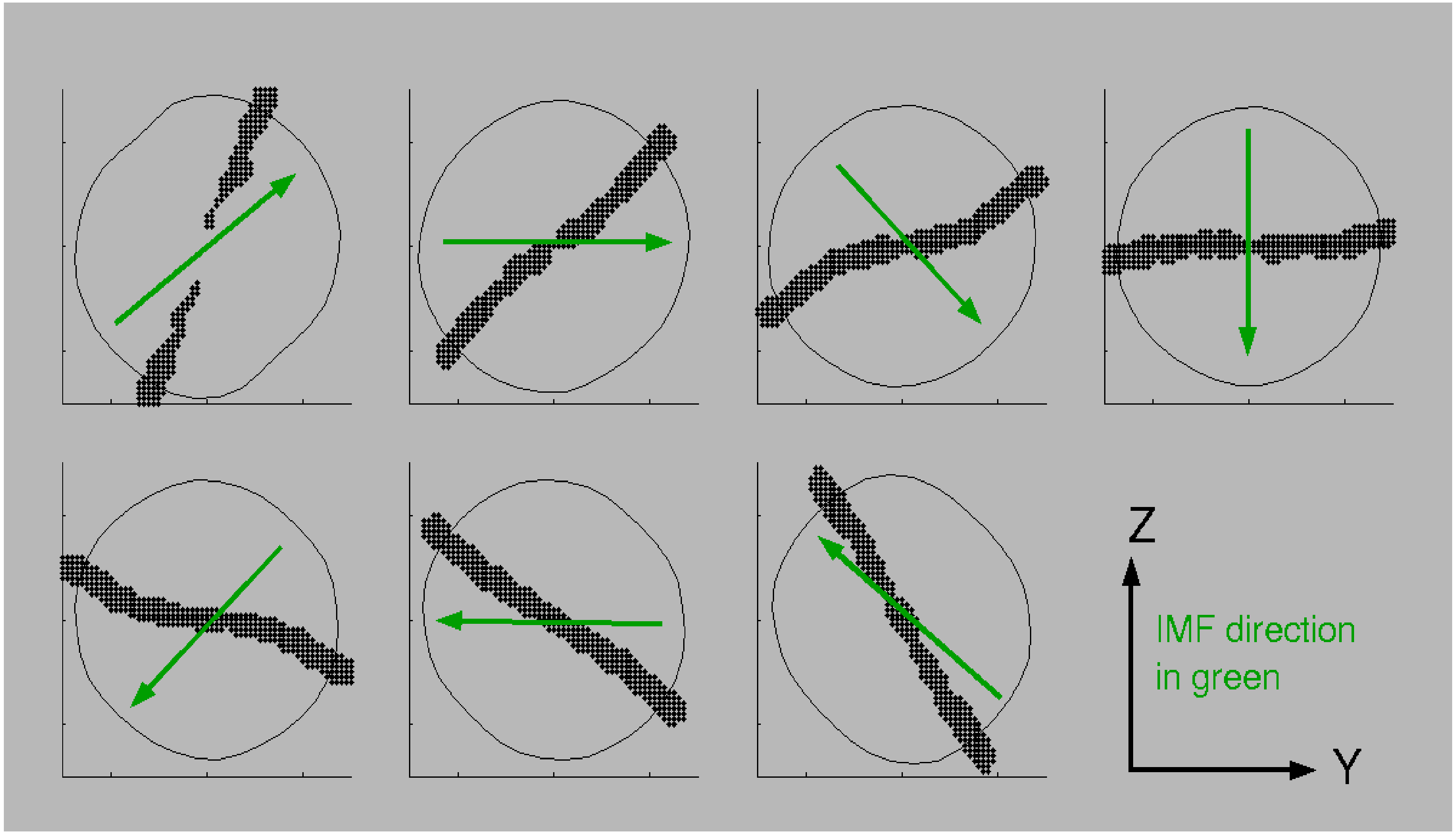

Association of reconnection and energy conversion

Sweet - Parker model:

- Inside diffusion region
  Poynting vector divergence

$$\nabla \cdot \mathbf{S} = - \frac{V_{Ai} B_i^2}{\mu_0 L}$$

- gives conversion from
  magnetic to plasma energy

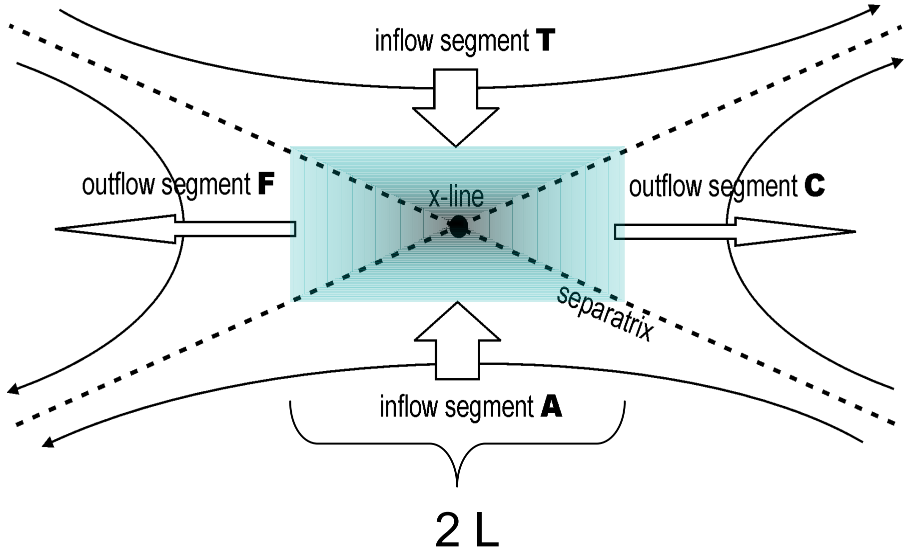

Energy conversion in the tail

Sweet - Parker -like reconnection in tail

- Magnetic annihilation surface density:

$$\sigma_{ann} = \int \nabla \cdot \mathbf{S} \, dl$$

- line integral across the diffusion region along the current sheet normal

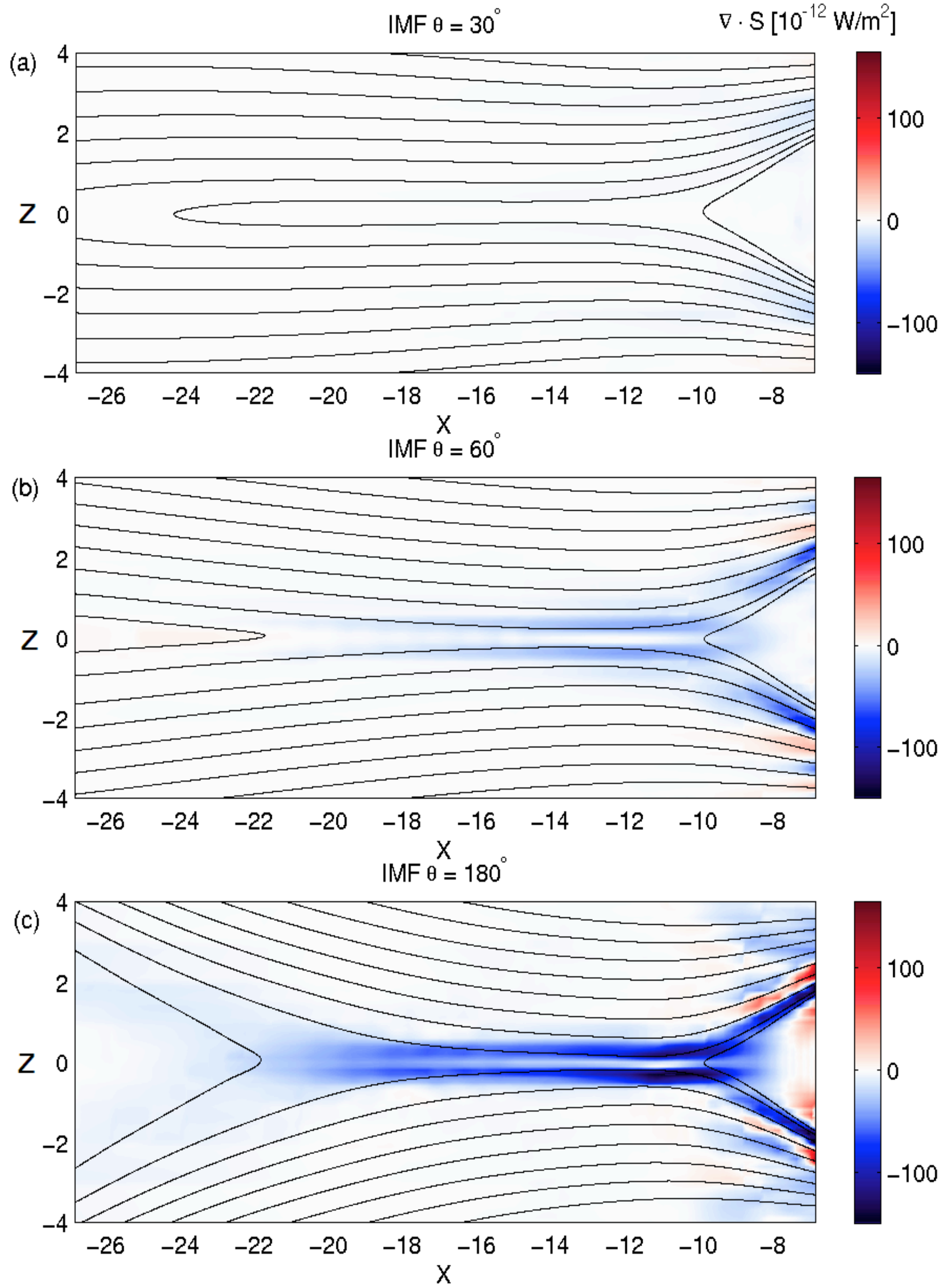

Energy conversion at magnetopause

Southward IMF:

- Strong magnetic annihilation at the nose (blue)
- Flux creation behind cusps (red)

Northward IMF:

- Only weak annihilation behind cusps

(Laitinen et al., 2006)

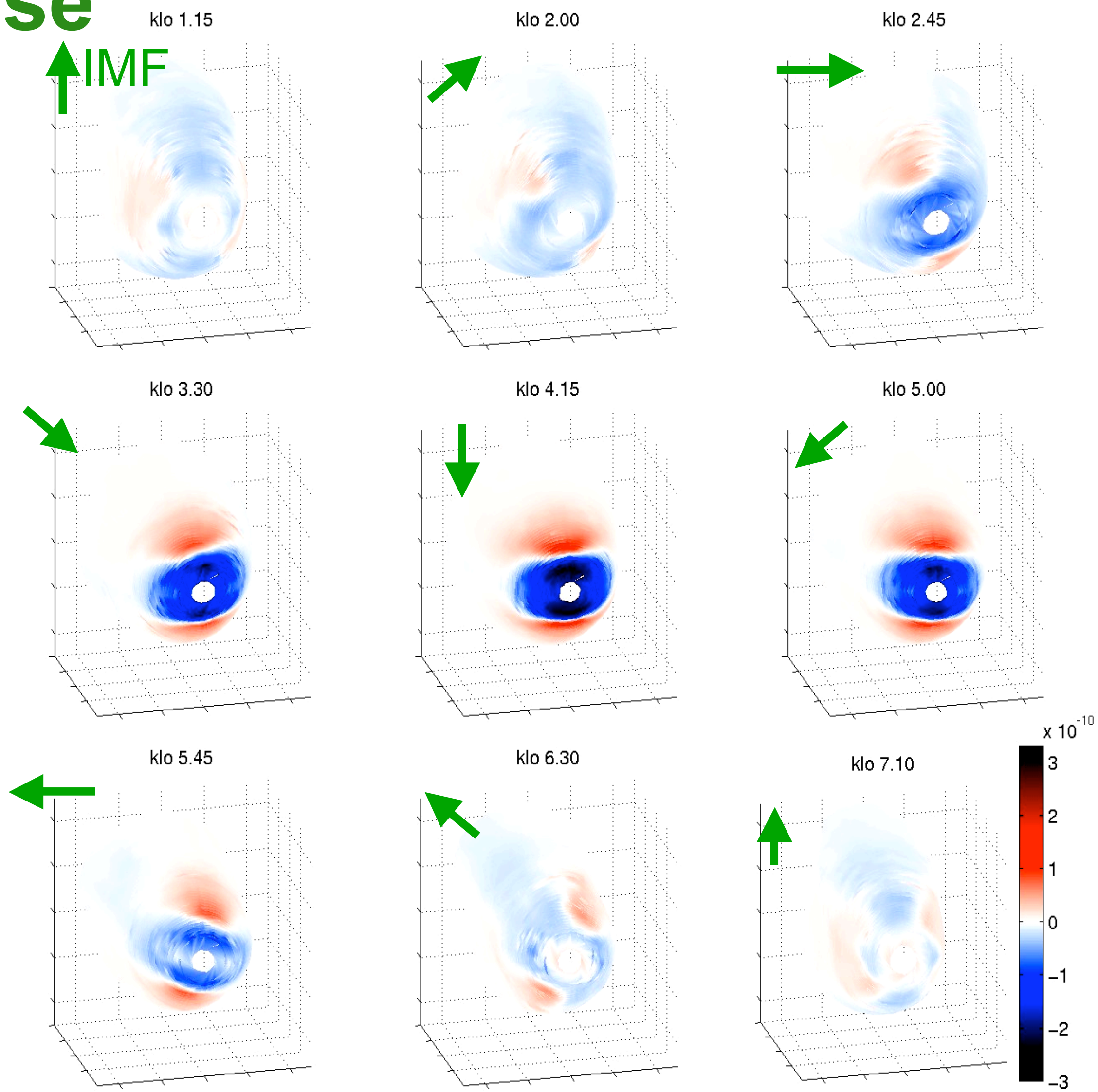

Energy conversion at magnetopause

Reconstruction power

- Volume integral of Poynting flux divergence

$$P_{rec} = \int \nabla \cdot \mathbf{S}\, dV$$

Annihilation at nose, dynamo behind cusps

- **blue**: reconnection power, X > 5
- **red**: dynamo power, 0 < X < 5

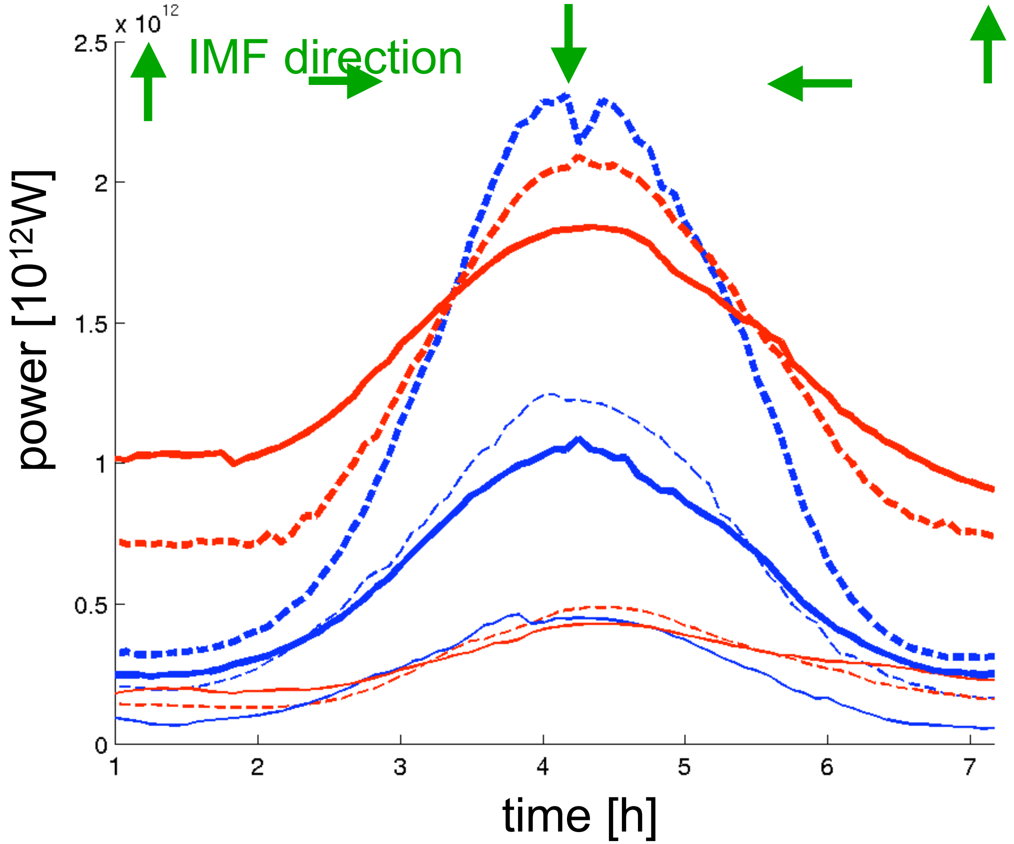

thick: Pdyn = 8 nPa
thin: Pdyn = 2 nPa

solid: |B| = 5 nT
dashed: |B| = 10 nT

Energy conversion in magnetotail

Reconnection power

- Volume integral of Poynting flux divergence

$$P_{rec} = \int \nabla \cdot \mathbf{S} \, dV$$

Reconnection drivers

- Pressure magnitude
- IMF orientation
- |B| has weaker effect
- Similar behavior at magnetopause and in tail

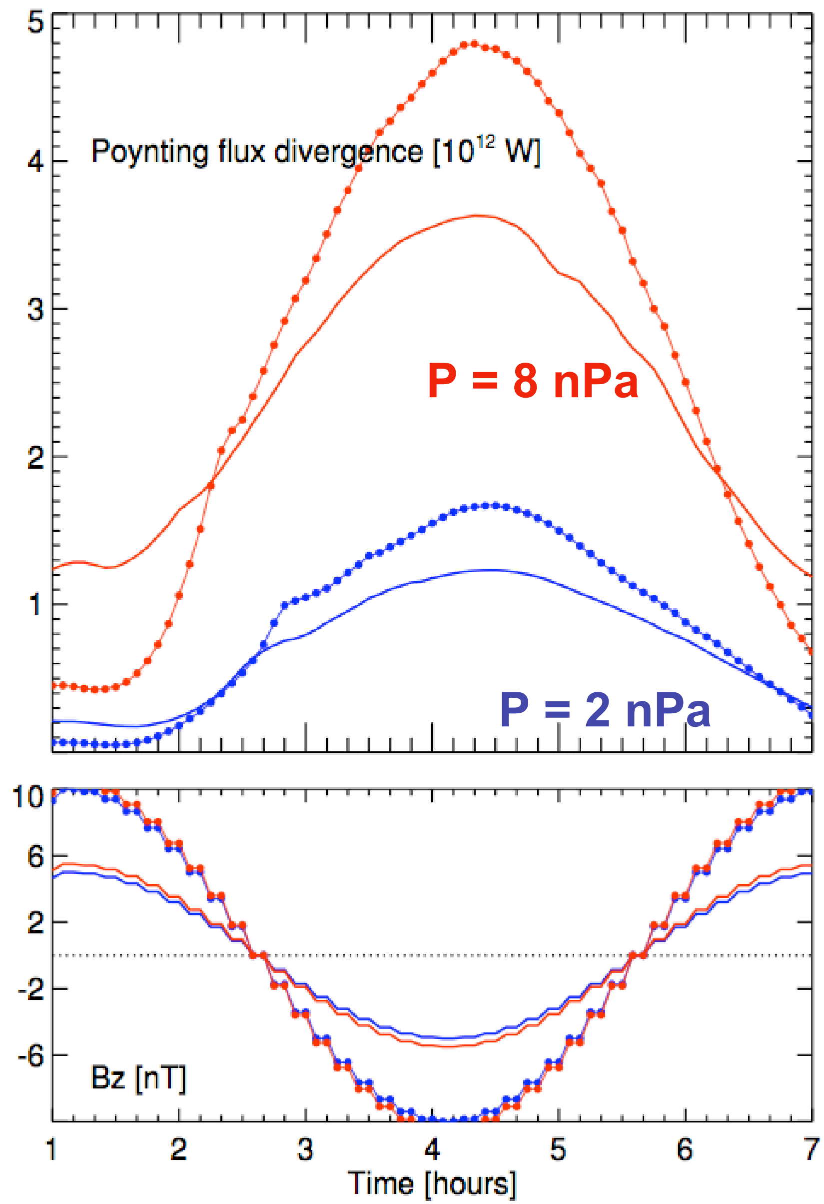

Ionospheric energy dissipation

GUMICS-4 Joule heating:

$$P_{JH} = \int \mathbf{E} \cdot \mathbf{J} \; dS = \int \Sigma_P E^2 \, dS$$

- Ionospheric electric field and conductivity

GUMICS-4 precipitation:

$$P_{PR} = \int (2/\pi m_e)^{1/2} n_e T_e^{3/2} dS$$

- Magnetospheric temperature and density

Joule heating

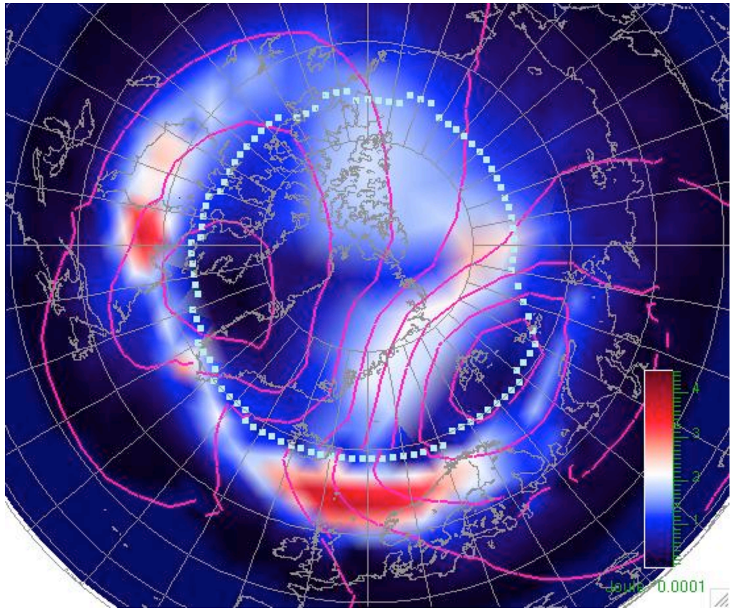

Precipitation energy

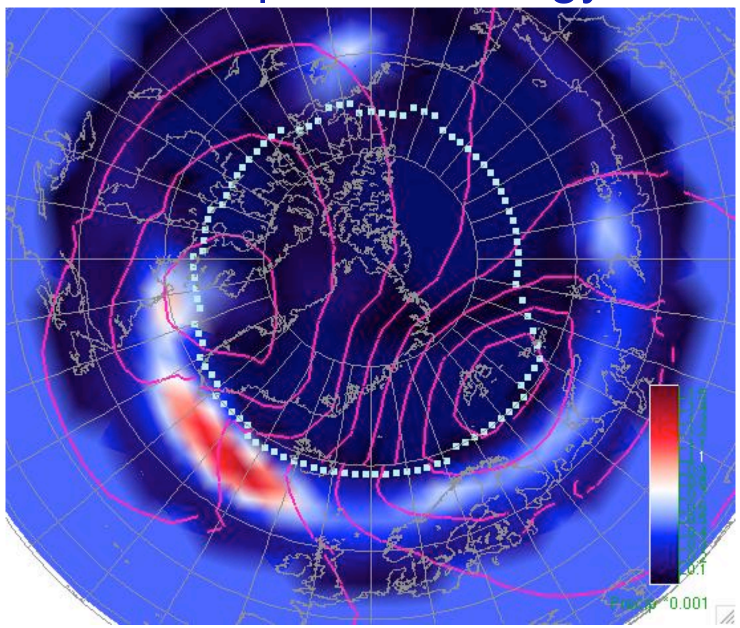

Ionospheric energy dissipation: Comparison with empirical proxy

Joule heat
(Ahn et al., 1983):

$P_{JH} = 2 \cdot 1.9 \cdot 10^8 \cdot AE$

Precipitation
(Ostgaard et al., 2002):

$P_{PR} = 2 \cdot 10^9 \, (4.4 \cdot AL^{1/2} - 7.6)$

Storm: April 6, 2000

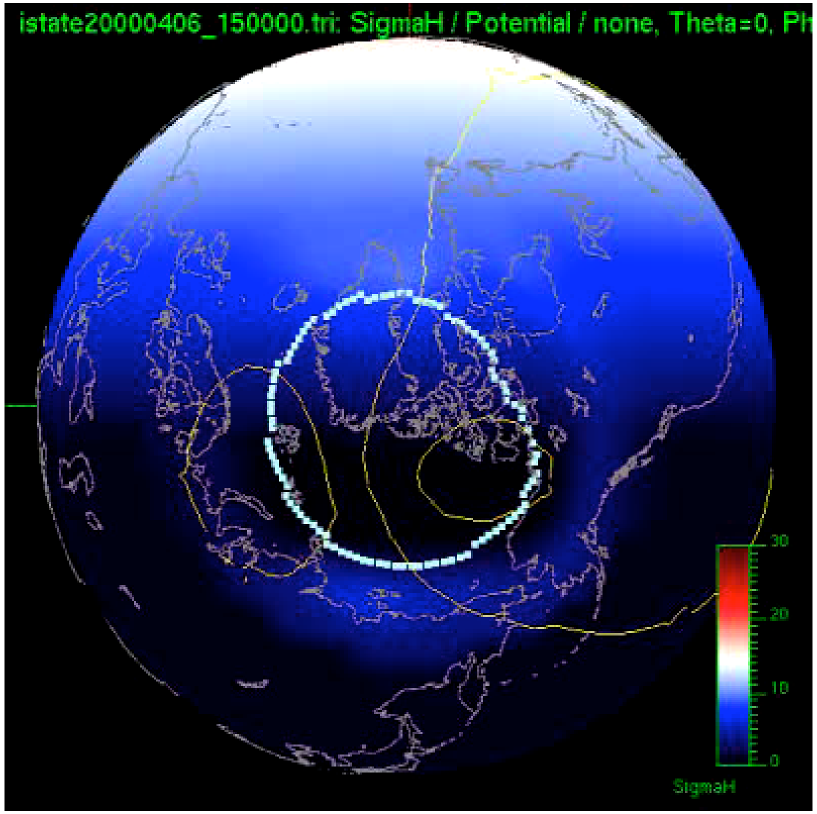

Ionospheric energy dissipation: Comparison with empirical proxy

Joule heat
(Ahn et al., 1983):

$P_{JH} = 2 \cdot 1.9 \cdot 10^8 \cdot AE$

Precipitation
(Ostgaard et al., 2002):

$P_{PR} = 2 \cdot 10^9 (4.4 \cdot AL^{1/2} - 7.6)$

Storm: April 6, 2000

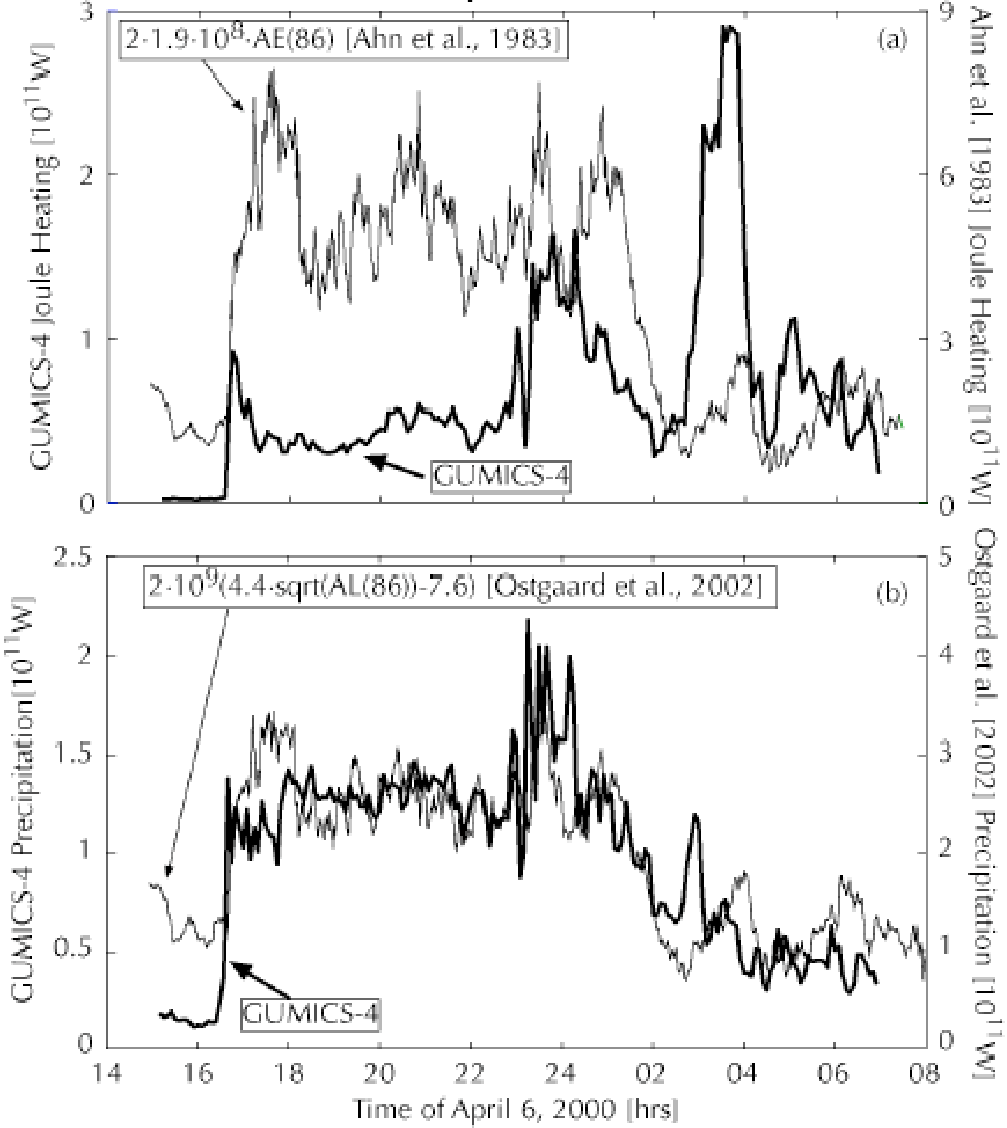

Ionospheric energy dissipation

- Joule heating and particle precipitation
- Driven by frontside reconnection (IMF Bz)
- Rate controlled by Psw

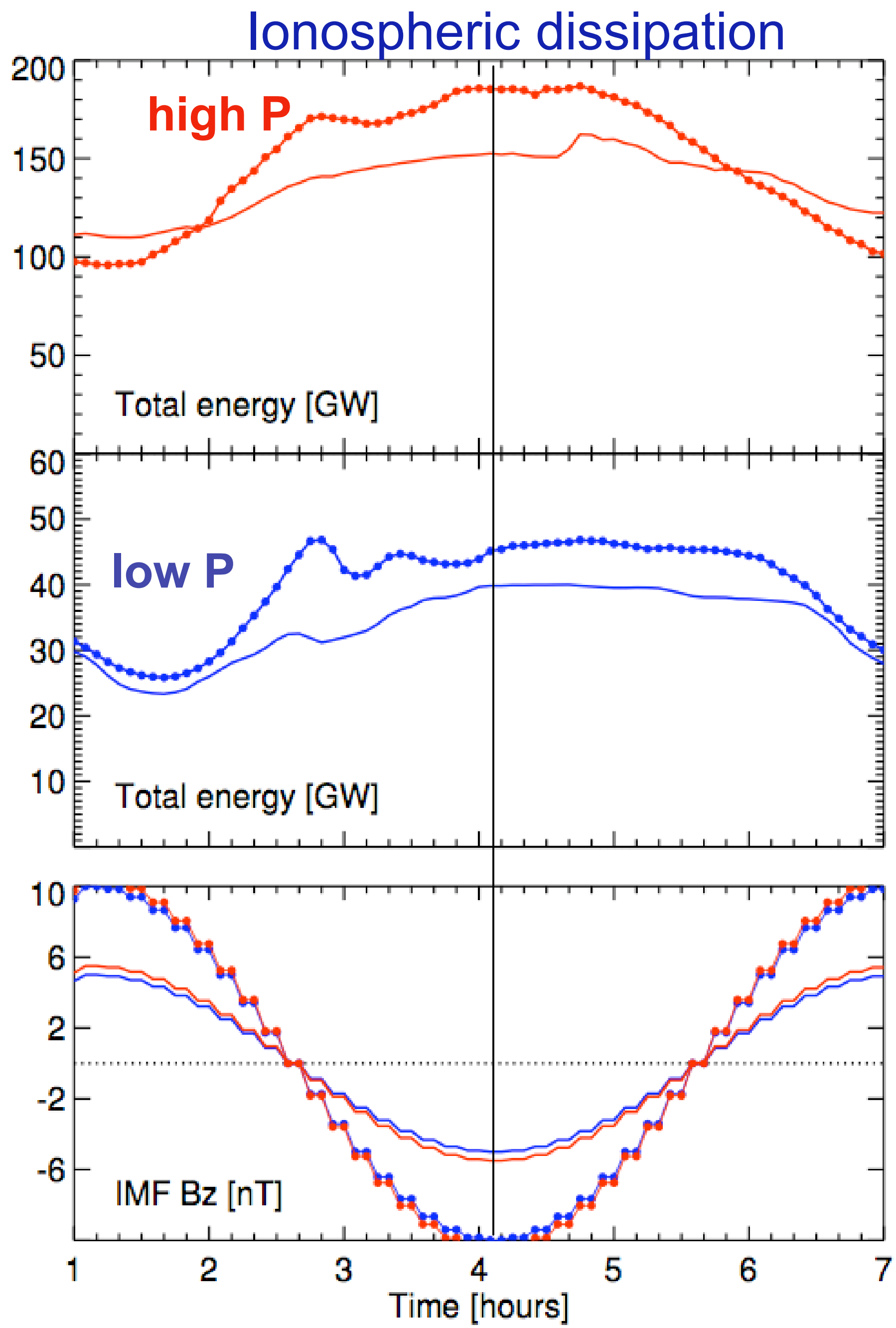

R1 and R2 field-aligned currents: solar wind pressure dependence

- Pressure controls size of magnetosphere and Chapman-Ferraro currents

- Chapman-Ferraro currents are linked to R1 currents

- R1 currents are linked to R2 currents

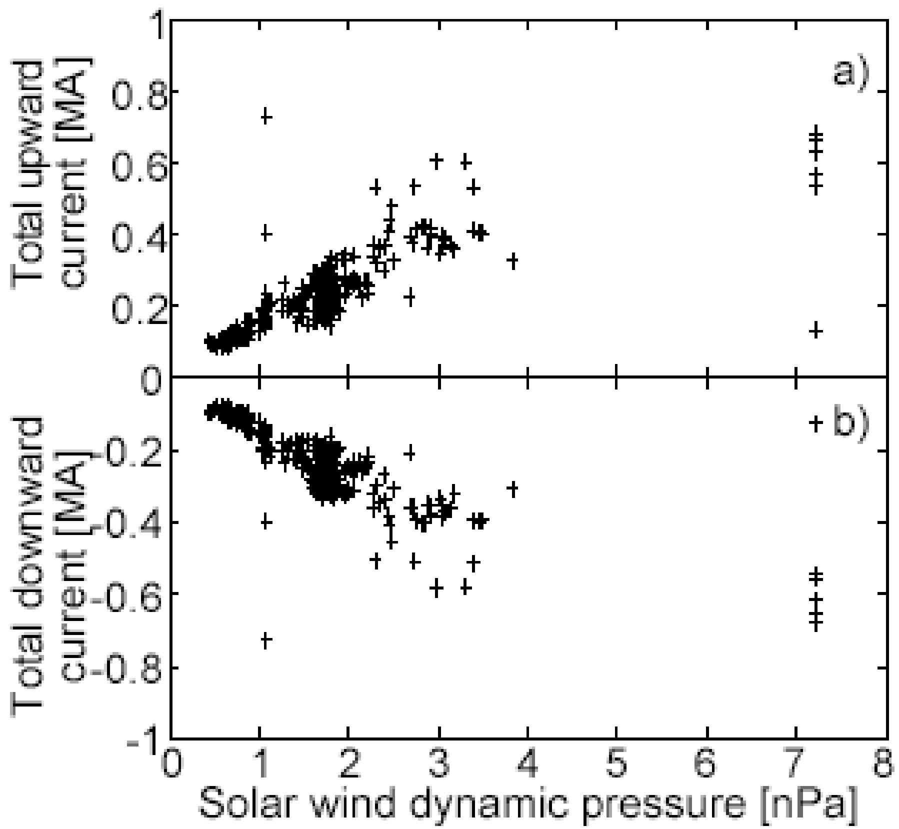

Ionospheric Joule heating: R1 and R2 dependence

- R1 currents close across polar cap
- R1 and R2 currents close across auroral oval
- Joule heating increases quadratically with increasing current (**P_{JH} ~ E·J ~ J^2/σ**)

(Palmroth et al., 2004)

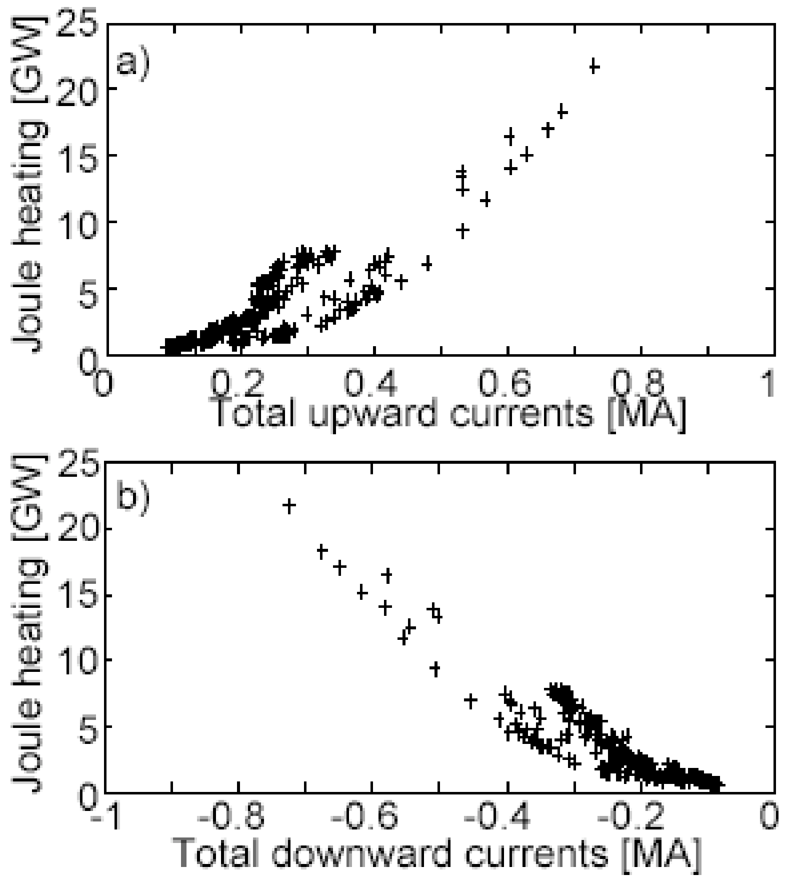

Ionospheric Joule heating: solar wind pressure dependence

- Solar wind pressure linearly correlated with ionospheric Joule heating
- Linear dependence different for **Bz > 0** and **Bz < 0**

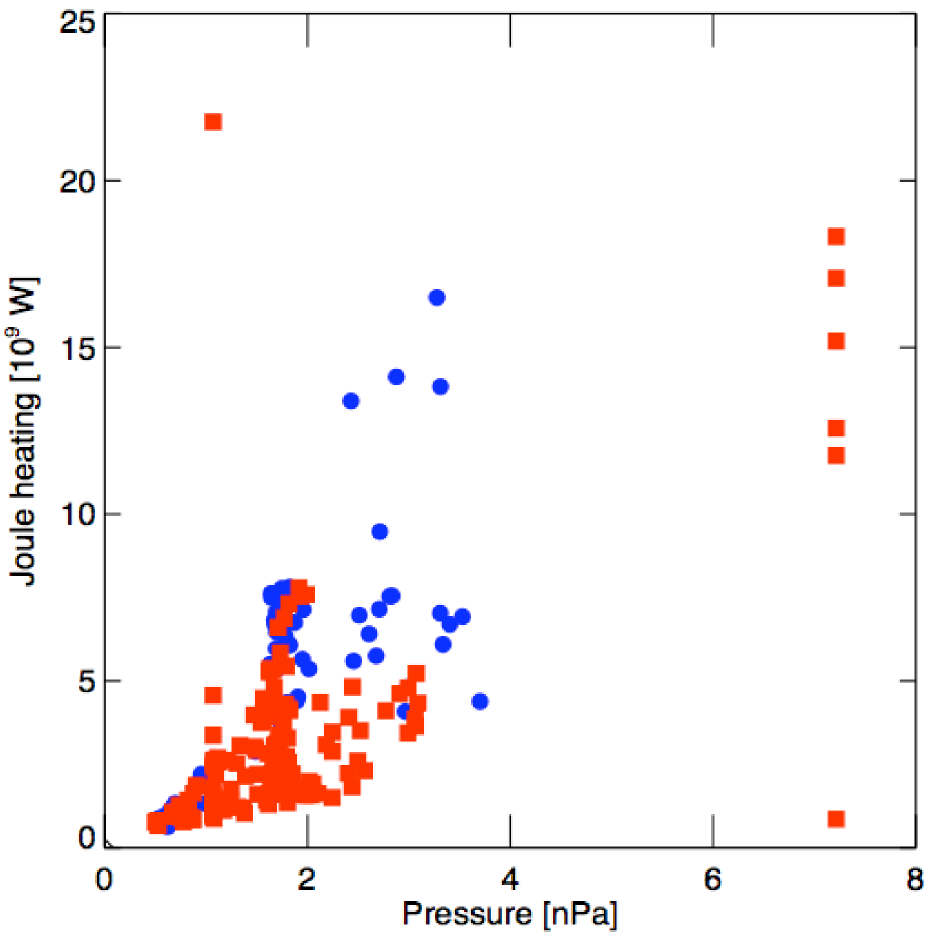

Ionospheric Joule heating:
solar wind pressure dependence

- Solar wind pressure correlated with ionospheric Joule heating
- Dependence different for Bz > 0 and Bz < 0

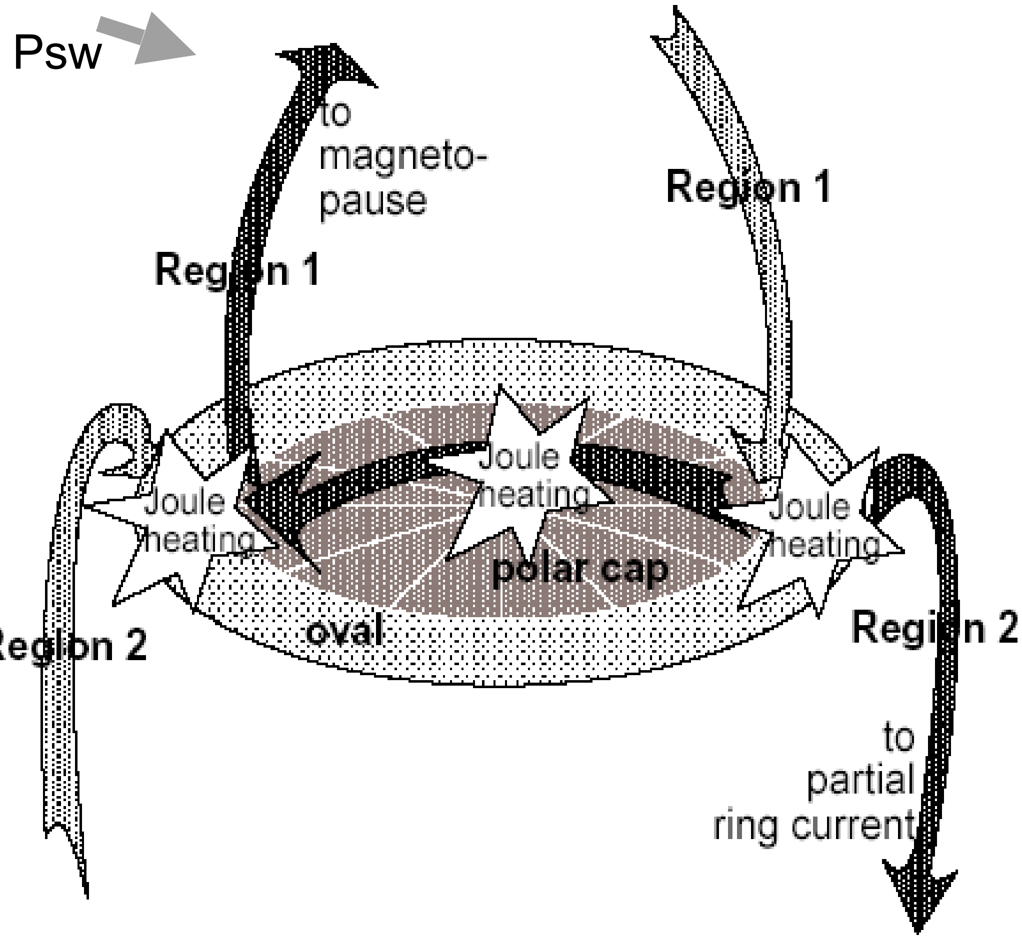

Ionospheric energy dissipation: Comparison with empirical proxy

Joule heat

(Ahn et al., 1983):

$P_{JH} = 2 \cdot 1.9 \cdot 10^8 \cdot AE$

Precipitation

(Ostgaard et al., 2002):

$P_{PR} = 2 \cdot 10^9 (4.4 \cdot AL^{1/2} - 7.6)$

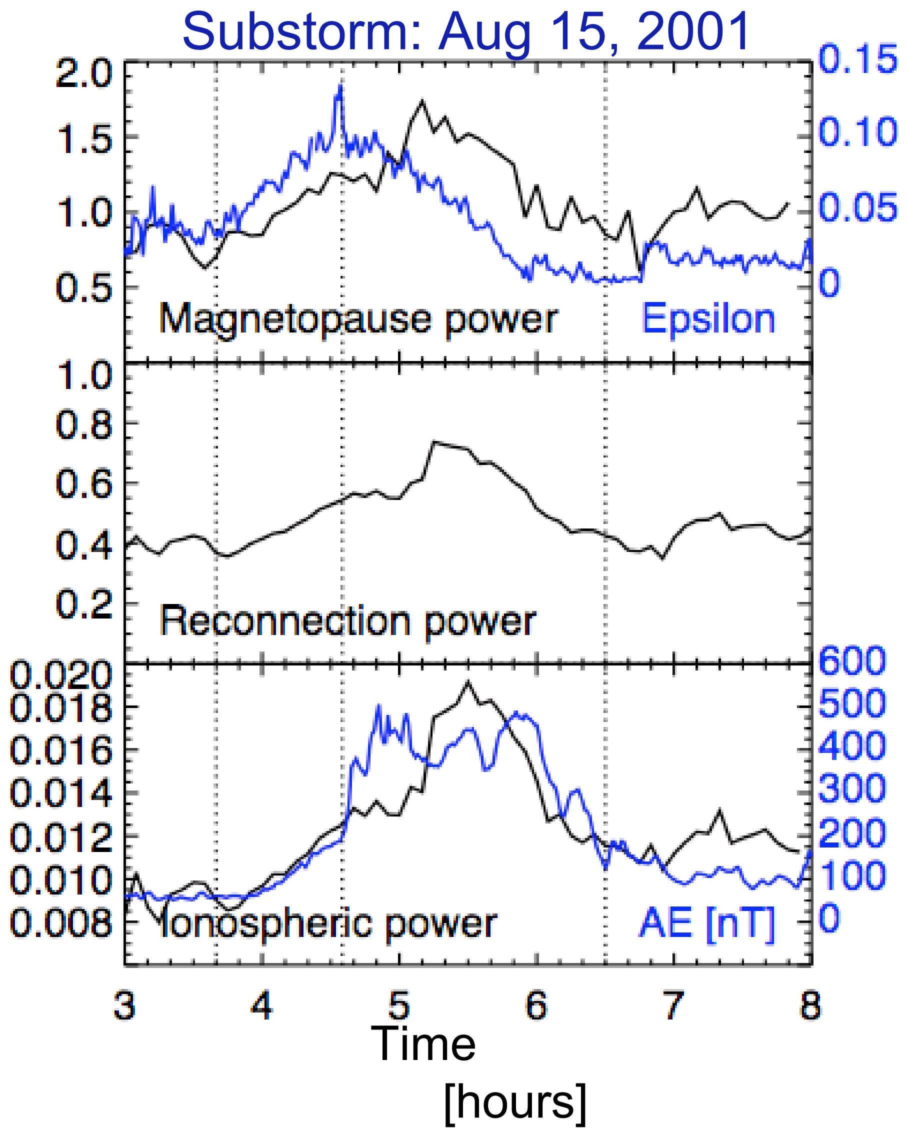

Power input: dependence on internal processes

Energy input to the magnetosphere - ionosphere:

- After quiet period:
  - Epsilon (or VB_Z) increase enhances energy input through magnetopause
- After previous driving:
  - Energy input continues even if Epsilon (or VB_Z) decreases

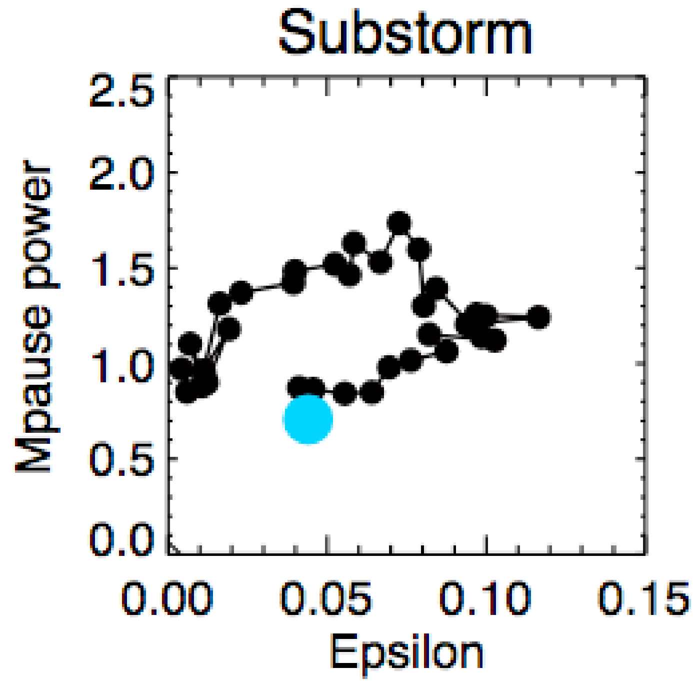

Ionospheric dissipation: direct dependence on energy input

Epsilon vs. ionospheric dissipation:

- Storage - release or
- Loading - unloading

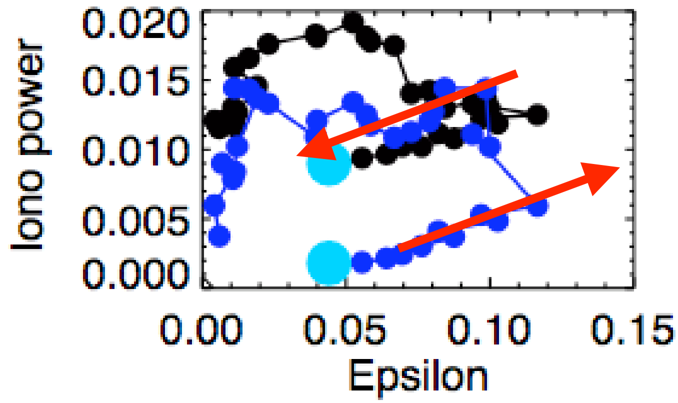

Traditional loading unloading cycle

Magnetopause input vs. ionospheric dissipation

- Direct driving

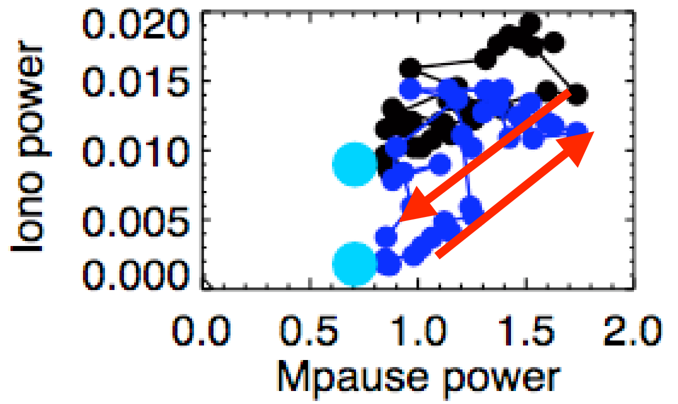

Directly driven cycle

(*Pulkkinen et al., 2006*)

Interpretation to substorm dynamics

Epsilon vs. ionospheric dissipation:

- Storage - release or
- Loading - unloading

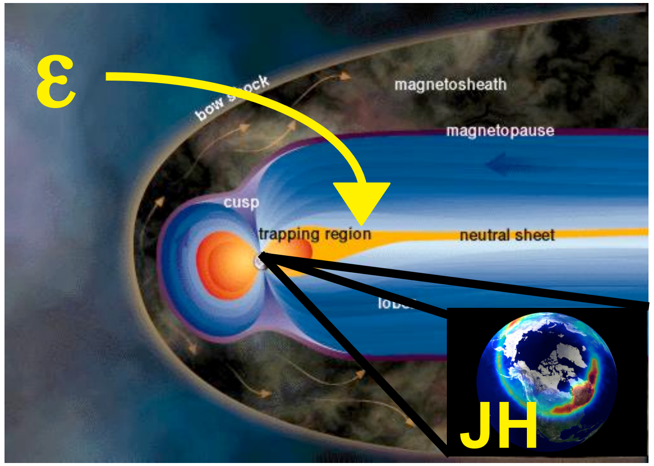

Magnetopause energy input vs ionospheric dissipation

- Direct driving

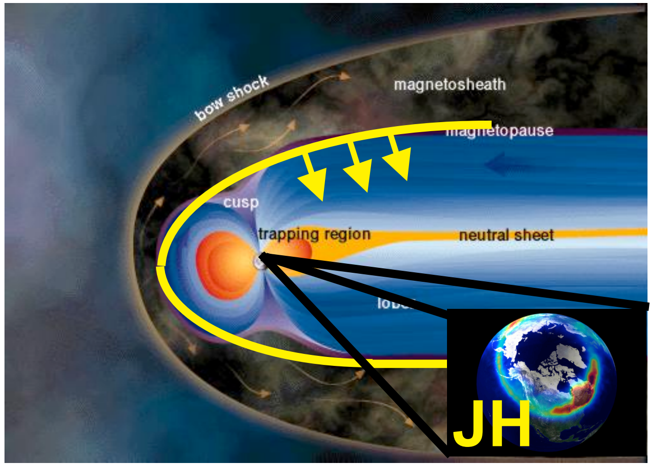

Effect of internal state

- Already at magnetopause!
- Not obtainable from observations!

Poynting flux focussing

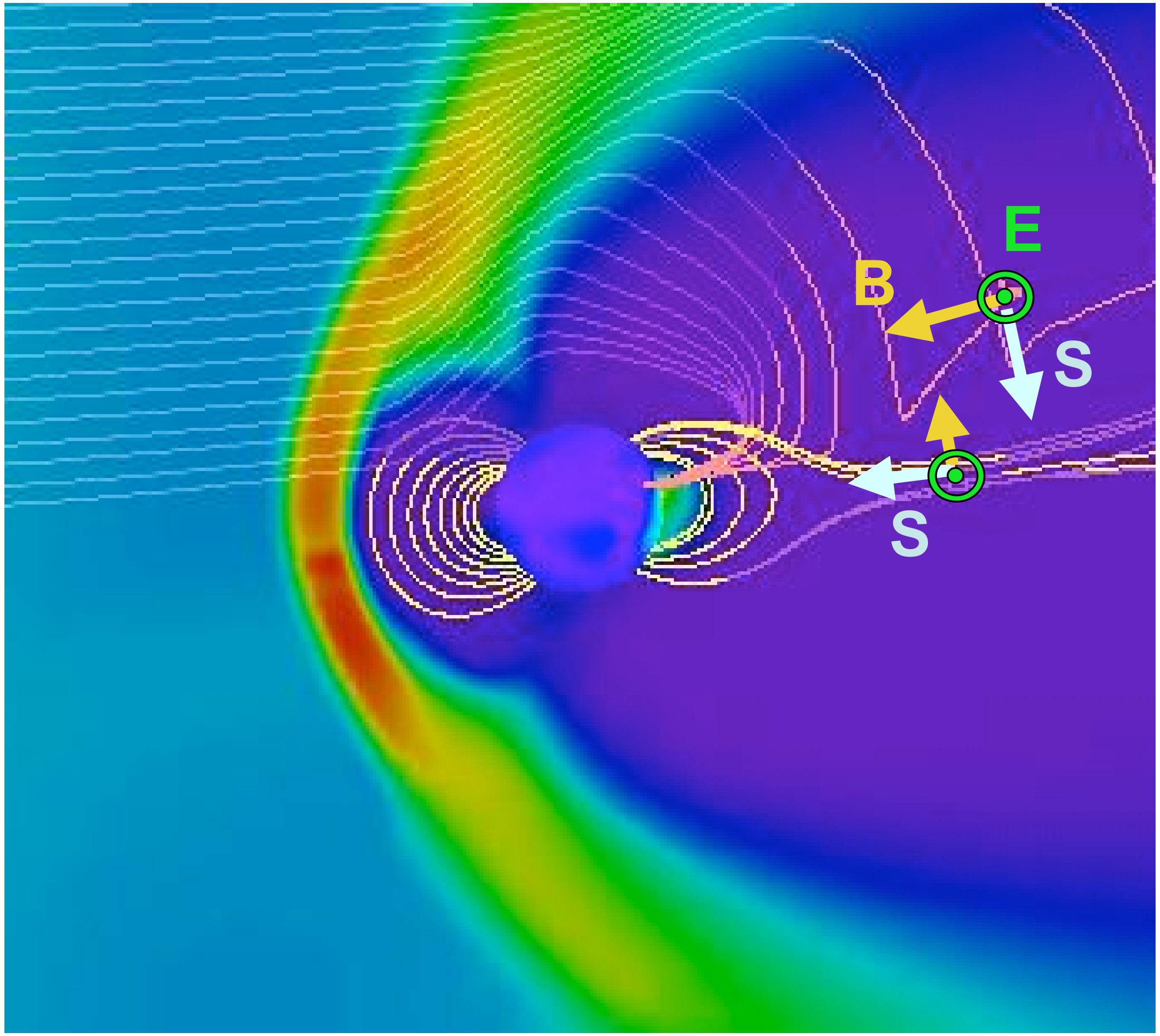

Summary and conclusions

Energy coupling

- Key to understanding reconnection and dynamics

MHD simulations

- Energy through magnetopause
- Energy conversion in tail follows energy input
- Energy dissipation in ionosphere follows energy input
- Poynting flux divergence couples reconnection and energy transport

Simulation results

- Component merging at magnetopause
- Poynting flux focusses in tail

Implications to MI coupling

- Pressure dependence on ionospheric Joule heating
- Ionospheric dissipation driven by solar wind input, which does not directly scale with epsilon